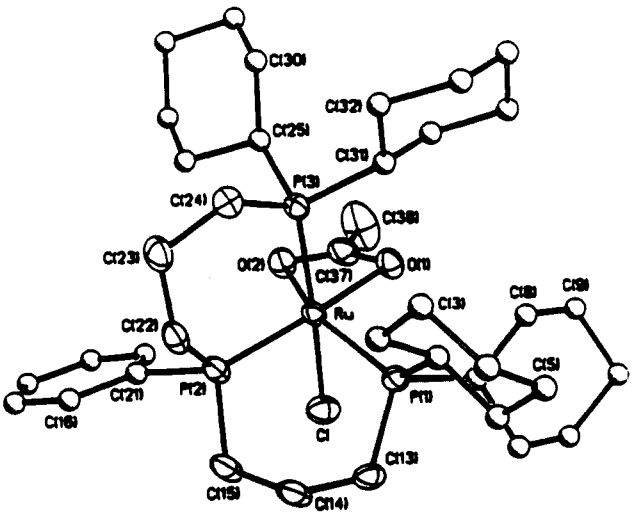

Figure 2. Molecular structure of *fac*-$RuCl(O_2CMe)(Cyttp)\cdot CH_3OH$. The solvent molecule and hydrogen atoms have been removed and the carbon atoms of the phenyl and cyclohexyl rings drawn as spheres with arbitrary radii for clarity. The thermal ellipsoids are drawn at the 40% probability level.

chelate acetate (58.9 (1)°). Such a small bite angle for the acetate ligand is normal and quite similar to those found in related ruthenium acetate complexes such as $RuH(O_2CMe)(PPh_3)_3$,[28] $Ru(O_2CMe)(p\text{-}MeC_6H_4NCH)(CO)(PPh_3)_2$,[29a] $[Ru(O_2CMe)(dppm)_2]BPh_4$,[29b] $[Ru(O_2CMe)(PMe_2Ph)_4]PF_6$,[29c] and $RuCl(O_2CMe)(CO)(PPh_3)_2$.[30] The acetate is coordinated in a symmetrical manner, as in analogous ruthenium complexes.[29b,c,30] The Ru–O bond distances (2.210 (3), 2.229 (3) Å) are in the range for reported values (e.g., 2.152 (6) and 2.144 (6) Å in $RuCl(O_2CMe)(CO)(PPh_3)_2$[30] and 2.173 (8) and 2.279 (8) Å in $Ru(O_2CMe)(p\text{-}MeC_6H_4NCH)(CO)(PPh_3)_2$[29a]). The Ru–P bond distances are very similar to those found in *fac*-$RuCl_2(Cyttp)$[16] and are in the range for the literature values.[31]

Discussion

It is interesting to note that *fac*-$RuCl(O_2CMe)(Cyttp)$ is more stable than *mer*-$RuCl(O_2CMe)(Cyttp)$, which gradually isomerizes into *fac*-$RuCl(O_2CMe)(Cyttp)$ in methanol, whereas *mer*-$RuH(O_2CMe)(Cyttp)$ is the only product of the reaction of $RuCl_2(Cyttp)$ with excess acetate in refluxing methanol under a hydrogen atmosphere. It appears that meridional complexes of Cyttp are usually favored due to steric interaction. Facial complexes could be more stable when there is a possibility that all the phosphorus atoms could be trans to weak trans-influence ligands to eliminate the trans phosphine interaction. The facial compound is more fluxional than the corresponding meridional isomer. For example, *fac*-$RuCl(O_2CMe)(Cyttp)$ and *fac*-$RuCl_2(Cyttp)$[16] are fluxional in dichloromethane at room temperature, whereas there is no evidence indicating that *mer*-$RuCl(O_2CMe)(Cyttp)$ and *mer*-$RuCl_2(Cyttp)$[16] are fluxional under similar conditions. The fluxionality is also dependent on solvents; for example, *fac*-$RuCl(O_2CMe)(Cyttp)$ is fluxional in dichloromethane but is rigid in benzene at room temperature. Complexes containing more than one carboxylate group are more fluxional than those with only one carboxylate group, as illustrated by the fluxional behavior of $Ru(O_2CMe)_2(ttp)$ and rigid behavior of $RuCl(O_2CMe)(ttp)$ in dichloromethane at room temperature.

Acknowledgment. We are grateful to the Johnson Mathey Co. for a loan of "$RuCl_3\cdot 3H_2O$". We thank Professors Robert H. Morris and Andrew Wojcicki for their help in the preparation of the manuscript.

Supplementary Material Available: Tables of crystallographic details and complete bond distances, bond angles, anisotropic thermal parameters, and coordinates and U values for hydrogen atoms (6 pages); a listing of observed and calculated structure factors (26 pages). Ordering information is given on any current masthead page.

(28) Skpski, A. C.; Stephens, F. A. *J. Chem. Soc., Dalton Trans.* **1974**, 390.
(29) (a) Clark, G. R.; Waters, J. M.; Whittle, K. R. *J. Chem. Soc., Dalton Trans.* **1975**, 2556. (b) Boyar, E. B.; Harding, P. A.; Robinson, S. D.; Brock, C. P. *J. Chem. Soc., Dalton Trans.* **1986**, 1771. (c) Ashworth, T. V.; Nolte, M. J.; Singleton, E. *J. Chem. Soc., Dalton Trans.* **1976**, 2184.
(30) Sanchez-Delgado, R. A.; Thewalt, U.; Valencia, N.; Andriollo, A.; Marquez-Silva, R.-L.; Puga, J.; Schollhorn, H.; Klein, H.-P.; Fontal, B. *Inorg. Chem.* **1986**, *25*, 1097.
(31) Jardine, F. H. *Prog. Inorg. Chem.* **1984**, *31*, 265.

Contribution from the Chemistry Department, University of Glasgow, Glasgow G12 8QQ, Scotland, and Department of Chemistry, University of Western Ontario, London, Canada N6A 5B7

A Fluxional Binuclear Nickel(I) Complex and Evidence for Reversible A-Frame Formation

Ljubica Manojlovic-Muir,*[1a] Kenneth W. Muir,[1a] William M. Davis,[1b] Hameed A. Mirza,[1b] and Richard J. Puddephatt*[1b]

Received May 15, 1991

The synthesis, structure, and fluxionality of the unusual dinickel(I) complex $[Ni_2Cl_2(\mu\text{-}CO)(\mu\text{-}dppm)_2]$ (**1a**), dppm = $Ph_2PCH_2PPh_2$, are described. Complex **1a** is formed by reaction of nickel(0) with nickel(II), in particular by reaction of $[Ni_2(CO)_2(\mu\text{-}CO)(\mu\text{-}dppm)_2]$ with $[NiCl_2(dppm)_2]$ or of $[Ni(CO)_2(dppm\text{-}P)_2]$ with $NiCl_2\cdot 6H_2O$. The crystal structure of **1a**·CH_2Cl_2 was determined by X-ray crystallography. [Space group $P2_1/n$, a = 13.890 (1) Å, b = 18.011 (1) Å, c = 19.614 (1) Å, β = 99.809 (4)°, Z = 4. The structure is based on 6722 reflections with $I \geq 3\sigma(I)$ and $4° \leq 2\theta(\text{Mo K}\alpha) \leq 54°$; 614 variables were refined to convergence at R = 0.038 and R_w = 0.051.] The molecular structure of **1a** contains a Ni–Ni bond of 2.617 (1) Å, a semibridging carbonyl and a trans,cis arrangement of the dppm ligands. The stereochemistries of the two nickel centers are therefore different, one being roughly square planar and the other roughly trigonal bipyramidal. However, in solution, the NMR spectra suggest a more symmetrical "A-frame" structure, and the data are rationalized in terms of a very easy fluxionality involving exchange of carbonyl between the nickel centers. Theoretical studies lend support to this hypothesis.

Introduction

The structures of certain d^9–d^9 dimers of the nickel group may exist in two structural forms as typefied by **1**, **3**, and **2**, **4**, respectively, in which LL is the binucleating ligand dppm ($Ph_2PCH_2PPh_2$) or dpam ($Ph_2AsCH_2AsPh_2$).

In the complexes **2** and **4** and several related "A-frame" complexes, there is no metal–metal bonding and each metal atom has square planar stereochemistry.[2] However, in **1**, **3**, and related

(1) (a) University of Glasgow. (b) University of Western Ontario.

0020-1669/92/1331-0904$03.00/0

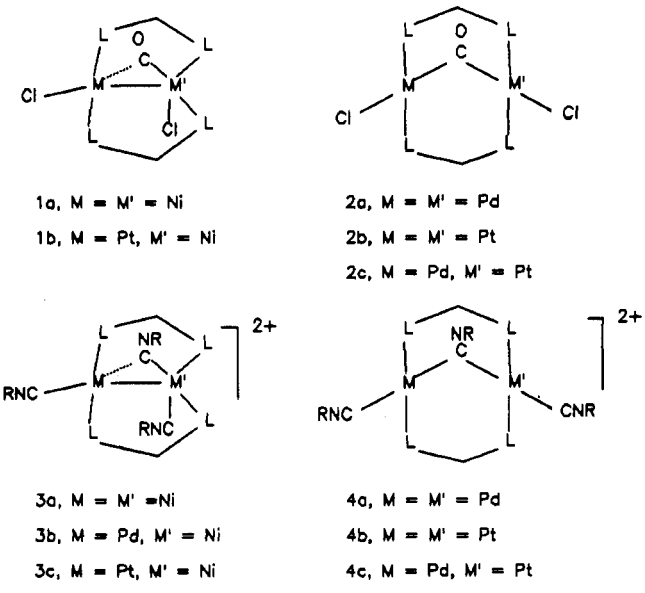

complexes the metal centers are not equivalent, and the metal–metal distance is in the range expected if there is a metal–metal bond.[3] These have been formulated as mixed oxidation state complexes with a coordinate metal–metal bond, formed by donation of an electron pair from a tetrahedral M(0) center to a T-shaped M(II) center.[3] In the nickel group, structure **1** or **3** has only been observed if one of the metal centers is nickel and, in heteronuclear complexes, the nickel is present as the tetrahedral Ni(0) donor M′ in **1** or **3**. The A-frame structure analogous to **2** or **4** has been found for nickel in $[Ni_2Cl_2(\mu\text{-SO})(\mu\text{-dppm})_2]$,[4] and it is not obvious why the different structures are adopted. This paper reports details of the synthesis and characterization of the complex $[Ni_2Cl_2(\mu\text{-CO})(\mu\text{-dppm})_2]$ (**1a**) and gives evidence for the easy interconversion between the structures **1** and **2**.[5]

Results and Discussion

Synthesis of Complex 1a. The complex $[Ni_2Cl_2(\mu\text{-CO})(\mu\text{-dppm})_2]$ (**1a**) was prepared by the reaction of the nickel(0) and nickel(II) complexes $[Ni_2(CO)_2(\mu\text{-CO})(\mu\text{-dppm})_2]$[6] and $[NiCl_2(dppm)_2]$,[7] according to eq 1.

$$[Ni_2(CO)_2(\mu\text{-CO})(\mu\text{-dppm})_2] + 2[NiCl_2(dppm)_2] \rightarrow 2[Ni_2Cl_2(\mu\text{-CO})(\mu\text{-dppm})_2] + 2dppm \quad (1)$$

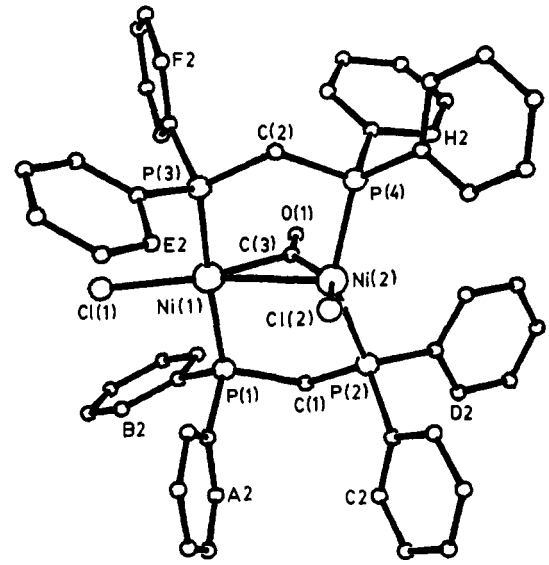

Figure 1. View of the molecular structure of complex **1a**. In the phenyl rings, carbon atoms are numbered cyclically, C(n1)...C(n6), where n = A–H and the C(n1) atoms are bonded to phosphorus. For clarity, only the C(n2) atoms are labeled by n2.

Table I. Selected Bond Lengths (Å) and Angles (deg) for $[Ni_2Cl_2(\mu\text{-CO})(\mu\text{-dppm})_2]$

Ni(1)–Ni(2)	2.617 (1)	Ni(1)–Cl(1)	2.225 (2)
Ni(1)–P(1)	2.231 (1)	Ni(1)–P(3)	2.242 (1)
Ni(1)–C(3)	1.926 (4)	Ni(2)–Cl(2)	2.262 (2)
Ni(2)–P(2)	2.221 (1)	Ni(2)–P(4)	2.214 (1)
Ni(2)–C(3)	1.790 (4)	P(1)–C(1)	1.848 (4)
P(1)–C(A1)	1.826 (4)	P(1)–C(B1)	1.825 (4)
P(2)–C(1)	1.844 (4)	P(2)–C(C1)	1.822 (4)
P(2)–C(D1)	1.824 (4)	P(3)–C(2)	1.861 (4)
P(3)–C(E1)	1.833 (4)	P(3)–C(F1)	1.826 (4)
P(4)–C(2)	1.844 (4)	P(4)–C(G1)	1.827 (4)
P(4)–C(H1)	1.820 (4)	O(1)–C(3)	1.177 (5)
Ni(2)–Ni(1)–Cl(1)	162.0 (1)	Ni(2)–Ni(1)–P(1)	88.3 (1)
Ni(2)–Ni(1)–P(3)	86.0 (1)	Ni(2)–Ni(1)–C(3)	43.1 (2)
Cl(1)–Ni(1)–P(1)	92.2 (1)	Cl(1)–Ni(1)–P(3)	91.3 (1)
Cl(1)–Ni(1)–C(3)	154.8 (2)	P(1)–Ni(1)–P(3)	171.6 (1)
P(1)–Ni(1)–C(3)	87.5 (2)	P(3)–Ni(1)–C(3)	92.5 (2)
Ni(1)–Ni(2)–Cl(2)	103.7 (1)	Ni(1)–Ni(2)–P(2)	102.2 (1)
Ni(1)–Ni(2)–P(4)	103.6 (1)	Ni(1)–Ni(2)–C(3)	47.4 (2)
Cl(2)–Ni(2)–P(2)	105.3 (1)	Cl(2)–Ni(2)–P(4)	92.6 (1)
Cl(2)–Ni(2)–C(3)	150.0 (2)	P(2)–Ni(2)–P(4)	144.0 (1)
P(2)–Ni(2)–C(3)	91.0 (2)	P(4)–Ni(2)–C(3)	88.2 (2)
Ni(1)–P(1)–C(1)	115.4 (2)	Ni(1)–P(1)–C(A1)	115.4 (2)
Ni(1)–P(1)–C(B1)	113.8 (2)	C(1)–P(1)–C(A1)	102.9 (2)
C(1)–P(1)–C(B1)	102.7 (2)	C(A1)–P(1)–C(B1)	105.1 (2)
Ni(2)–P(2)–C(1)	107.4 (2)	Ni(2)–P(2)–C(C1)	122.7 (2)
Ni(2)–P(2)–C(D1)	115.1 (2)	C(1)–P(2)–C(C1)	106.7 (2)
C(1)–P(2)–C(D1)	102.0 (2)	C(C1)–P(2)–C(D1)	100.8 (2)
Ni(1)–P(3)–C(2)	119.8 (2)	Ni(1)–P(3)–C(E1)	110.9 (2)
Ni(1)–P(3)–C(F1)	113.6 (2)	C(2)–P(3)–C(E1)	102.2 (2)
C(2)–P(3)–C(F1)	102.5 (2)	C(E1)–P(3)–C(F1)	106.4 (2)
Ni(2)–P(4)–C(2)	101.4 (2)	Ni(2)–P(4)–C(G1)	124.5 (2)
Ni(2)–P(4)–C(H1)	118.9 (2)	C(2)–P(4)–C(G1)	102.6 (2)
C(2)–P(4)–C(H1)	108.0 (2)	C(G1)–P(4)–C(H1)	99.6 (2)
P(1)–C(1)–P(2)	110.6 (2)	P(3)–C(2)–P(4)	114.2 (2)
Ni(1)–C(3)–Ni(2)	89.5 (2)	Ni(1)–C(3)–O(1)	122.4 (3)
Ni(2)–C(3)–O(1)	148.2 (3)		

Complex **1a** was also obtained by reaction of $[Ni(CO)_2(dppm\text{-}P)_2]$ with nickel(II) chloride. Both synthetic methods are variations of reaction of Ni(0) with Ni(II) to give 2Ni(I).

The complex **1a** was obtained as deep green-black crystals. Solutions or powdered samples of **1a** are green, while large crystals appear black. In solution the complex was very sensitive to oxygen, but the solid complex was oxidized more slowly by air.

Structure of 1a. The structure of the product was determined by an X-ray crystal structure analysis of its solvate **1a**·CH_2Cl_2. The molecular structure of **1a** is shown in Figure 1 and is char-

(2) (a) Colton, R.; McCormick, M. J.; Pannan, C. D. *Aust. J. Chem.* **1978**, *31*, 1425. (b) Brown, M. P.; Keith, A. N.; Manojlovic-Muir, Lj.; Muir, K. W.; Puddephatt, R. J.; Seddon, K. R. *Inorg. Chim. Acta* **1979**, *34*, L223. (c) Pringle, P. G.; Shaw, B. L. *J. Chem. Soc., Dalton Trans.* **1983**, 889. (d) Lee, C.-L.; James, B. R.; Nelson, D. A.; Hallen, R. T. *Organometallics* **1984**, *3*, 1360. (e) Benner, L. S.; Balch, A. L. *J. Am. Chem. Soc.* **1978**, *100*, 6099. (f) Brown, M. P.; Puddephatt, R. J.; Rashidi, M.; Seddon, K. R. *J. Chem. Soc., Dalton Trans.* **1978**, 1540. (g) Grundy, K. R.; Robertson, K. N. *Organometallics* **1983**, *2*, 1736.

(3) (a) Holah, D. G.; Hughes, A. N.; Magneson, V. R.; Mirza, H. A.; Parker, K. O. *Organometallics* **1988**, *7*, 1233. (b) Ratliff, K. S.; Fanwick, P. E.; Kubiak, C. P. *Polyhedron* **1990**, *9*, 2651. (c) DeLaet, D. L.; del Rosario, R.; Fanwick, P. E.; Kubiak, C. P. *J. Am. Chem. Soc.* **1987**, *109*, 754. (d) Ni, J.; Kubiak, C. P. *Inorg. Chem.* **1990**, *29*, 4345. (e) Ni, J.; Fanwick, P. E.; Kubiak, C. P. *Inorg. Chem.* **1988**, *27*, 2020.

(4) Gong, J. K.; Fanwick, P. E.; Kubiak, C. P. *J. Chem. Soc., Chem. Commun.* **1990**, 1190.

(5) After this work was completed we learned that Kubiak and co-workers had reported complex **1a** in a conference abstract. There is agreement on the structure of **1a** [Ni–Ni = 2.614 (2) Å, compared to 2.617 (1) Å in the present work] but not on the magnetic properties. We thank Dr. C. P. Kubiak for several helpful discussions. Gong, J. K.; Morgenstern, D.; Fanwick, P. E.; Kubiak, C. P. *Abstracts of Papers*, 198th National Meeting of the American Chemical Society, Miami Beach, FL; American Chemical Society: Washington, DC, 1989; Abstr 281, mentioned in ref 4.

(6) (a) Holah, D. G.; Hughes, A. N.; Mirza, H. A.; Thompson, J. D. *Inorg. Chim. Acta* **1987**, *126*, L7. (b) Zhang, Z.-Z.; Wang, H.-K.; Wang, H.-G.; Wang, R.-J.; Zhao, W.-J.; Yang, L.-M. *J. Organomet. Chem.* **1988**, *347*, 269. (c) Osborn, J. A.; Stanley, G. G.; Bird, P. H. *J. Am. Chem. Soc.* **1988**, *110*, 2117.

(7) Van Hecke, G. R.; Horrocks, W. D., Jr. *Inorg. Chem.* **1966**, *5*, 1968.

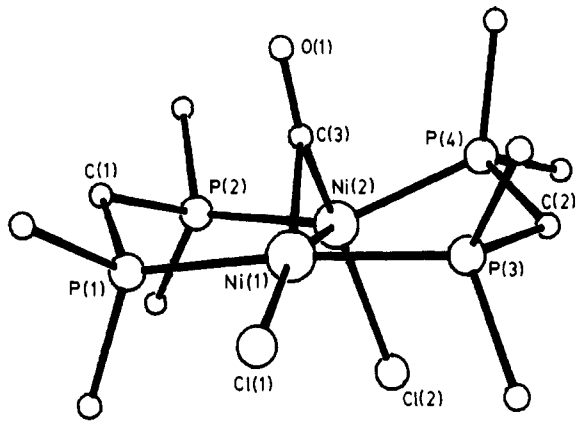

Figure 2. Molecular structure of **1a** viewed approximately along the Ni–Ni bond. The phenyl carbon atoms are omitted except those bonded to phosphorus.

acterized by bond lengths and angles listed in Table I. It comprises two NiCl fragments held together by an unsymmetrically bridging carbonyl [Ni(2)–C(3) = 1.790 (4), Ni(1)–C(3) = 1.926 (4) Å; Ni(1)–C(3)–Ni(2) = 89.5 (2)°] and by two bridging dppm ligands. These dppm ligands adopt a trans,cis configuration around the two metal centers. The NiCl fragments are also linked directly by a Ni–Ni bond [2.617 (1) Å] comparable in length with the metal–metal single bonds observed in other dppm-bridged dinickel complexes [Ni–Ni = 2.439 (1)–2.694 (1) Å].[3,5,6,8] The two five-membered Ni_2P_2C rings adopt distorted envelope conformations as shown in Figure 2. The metal atoms display different coordination geometries. Around the Ni(1) atom the geometry is approximately square planar, with one coordination site spanned by the Ni(2)–C(3) bond. The geometry around the Ni(2) atom can be described as highly distorted trigonal bipyramidal, with the Ni(1), P(2), and P(4) atoms at equatorial and the Cl(2) and C(3) atoms at axial sites.

The complex **1a** is therefore isostructural with **1b** and **3a**, in which the bridging CO [Pt–C = 2.03 (1), Ni–C = 1.77 (2) Å; Ni–C–O = 145 (1)°] or bridging MeNC [Ni–μ-C = 2.19 (1), 1.824 (9) Å] is considered semibridging.[3a,c] The structure of **1a** is also similar to those of the complexes $[RhM(CO)_2(\mu\text{-}CO)(\mu\text{-}dppm)_2]$, M = Rh, Ir, or Co,[9] into which it would transform by a Berry pseudorotation interchanging the positions of the equatorial Ni–Ni and axial Ni–μ-C bonds around Ni(2).

Complex **1a** can be considered to be formed from $[Ni_2(CO)_2(\mu\text{-}CO)(\mu\text{-}dppm)_2]$ (**5**) by a 2-electron oxidation with substitution of the terminal carbonyl groups in **5** by chloride ligands but with retention of the μ-CO group. Opening of the P–Ni–P angles from 106° in **5** to 172 and 142° in **1a**[6] leads to conversion of the cis,cis W-frame[10] or cradle type structure[3,6,8] of **5** into the trans,cis structure of **1a**. The major difference between the structures of **1a** and its palladium and platinum congeners,[2] which have symmetrical A-frame structures, has been mentioned above.

Spectroscopic Properties of Complex 1a. The carbonyl stretching frequency in the IR spectrum of **1a** was at 1763 cm^{-1} in the solid state and at 1765 cm^{-1} in CH_2Cl_2 solution. The close similarity indicates that the solid-state structure with a semibridging carbonyl ligand is retained in solution. For comparison the ν(CO) values for **2a** and **2b** are 1705 and 1638 cm^{-1}, respectively.[2] In the nickel group, back-bonding is usually weakest for palladium so the higher value of ν(CO) for the nickel complex can be attributed to the different structures, with the ketonic carbonyls in **2** giving lower ν(CO) values than the semibridging carbonyl in **1a** [ν(CO) = 1763 cm^{-1}] or **1b** [ν(CO) 1756 cm^{-1}]. The FAB mass spectrum of **1a** gave an envelope of peaks centered at m/e = 925 corresponding to $(M + H)^+$ (figures given for ^{35}Cl and ^{58}Ni isotopes), and the most intense envelope was at m/e = 889 corresponding to $(M - Cl)^+$. There was no peak corresponding to loss of CO from **1a**, indicating that the carbonyl group is strongly bound. This is consistent with our observation that CO is not easily lost from **1a** by thermolysis, whereas similar heating of **2a** or **2b** easily gives CO and $[M_2Cl_2(\mu\text{-}dppm)_2]$.[2]

The ^{31}P NMR spectrum of **1a** gives a singlet at δ = 17.1 at 20 °C, and this shifts only slightly to δ = 17.7 ppm at −90 °C in CH_2Cl_2 solution. Since the ground-state structure (Figure 1) has two very different phosphorus environments, it is clear that the complex must be fluxional even at low temperature. Some further information is obtained from the ^1H NMR spectra. At 20 °C the CH_2P_2 protons of the dppm ligands gave an "AB" pattern [$\delta(H^a)$ 2.96, $\delta(H^b)$ 3.33, $^2J(H^aH^b)$ = 14 Hz], with further unresolved splitting due to $^{31}P^1H$ coupling, and the spectrum was essentially the same at −90 °C. These data show that the fluxionality creates an effective plane of symmetry perpendicular to the Ni–Ni axis, thus making the two nickel atoms and four phosphorus atoms equivalent, but does not create a plane of symmetry containing the $Ni_2P_4C_2$ skeleton. Hence, the NMR properties are those expected for an A-frame structure **2**,[2] and the fluxional process is defined as the carbonyl migrating between the nickel atoms, with accompanying changes in stereochemistry at each nickel, as shown in eq 2, perhaps by way of the A-frame structure **2**.

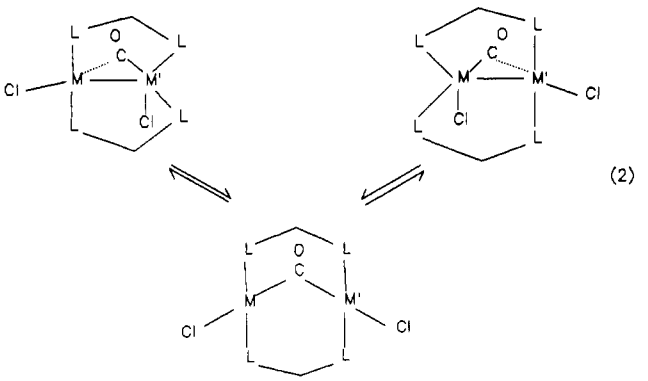

The NMR data indicate that **1a** is diamagnetic, and this has been confirmed for solutions in CH_2Cl_2 both at +20 and at −90 °C by the Evans method.[11] In the solid state, the complex is diamagnetic at 20 °C (Gouy method) with $\chi_M = -6 \times 10^{-5}$ cgs units, but after allowance for the diamagnetic susceptibility of the ligands, there does appear to be a weak paramagnetic contribution from the nickel atoms. The solid complex also gives a broad, ill-defined EPR signal. It is suspected that the weak paramagnetism is due to partial oxidation of the air-sensitive compound, but the possibility that there is a low-spin/high-spin equilibrium involved cannot be eliminated.

Theoretical Studies on 1a. There have been several studies of bonding in dppm-bridged dimers, including $[M_2X_2(\mu\text{-}dppm)_2]$ and their derivatives of the A-frame type.[10,12,13] In the present work, the dppm ligands have been substituted by carbonyl ligands. This is, of course, a gross approximation which is justified by the need to modify the distances and angles between donor atoms in order to model both structures **1** and **2**, which would lead to complications if a model bidentate ligand such as $H_2PCH_2PH_2$ or multiatom ligand such as PH_3 were used to model the dppm donors. The results will only be used in a qualitative way.

(8) (a) Einspahr, H.; Donohue, J. *Inorg. Chem.* **1974**, *13*, 1839. (b) DeLaet, D. L.; Powell, D. R.; Kubiak, C. P. *Organometallics* **1985**, *4*, 954. (c) DeLaet, D. L.; Fanwick, P. E.; Kubiak, C. P. *Organometallics* **1986**, *5*, 1807.

(9) (a) Woodcock, C.; Eisenberg, R. *Inorg. Chem.* **1985**, *24*, 1285. (b) McDonald, R.; Cowie, M. *Inorg. Chem.* **1990**, *29*, 1564. (c) Elliot, D. J.; Ferguson, G.; Holah, D. G.; Hughes, A. N.; Jennings, M. C.; Magnuson, V. R.; Potter, D.; Puddephatt, R. J. *Organometallics* **1990**, *9*, 1336.

(10) Karsch, H. H.; Milewski-Mahrla, B.; Besenhard, J. O.; Hofmann, P.; Stauffert, P.; Albright, T. A. *Inorg. Chem.* **1986**, *25*, 3811.

(11) Evans, D. F. *J. Chem. Soc.* **1959**, 2003.

(12) Hoffman, D. M.; Hoffmann, R. *Inorg. Chem.* **1981**, *20*, 3543.

(13) Ratliff, K. S.; DeLaet, D. L.; Gao, J.; Fanwick, P. E.; Kubiak, C. P. *Inorg. Chem.* **1990**, *29*, 4022.

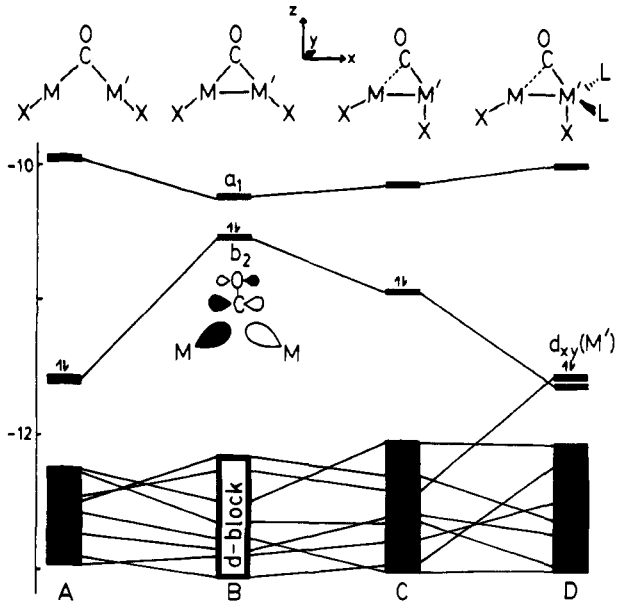

Figure 3. Key orbital energy changes as complex B undergoes distortion toward the stable structures A and D. (In the structures the ligands L = CO, substituting for dppm donor atoms, lying along the *y*-axis at 90° to the M–M′ axis are omitted for clarity.) The major factor influencing overall stability is the energy of the HOMO (b_2 in B). Values in the figure are for M, M′ = Pt, but the trend is very similar for M, M′ = Ni.

The formation of complexes **1** or **2** can be modeled in a number of ways. When M = Pt or Pd, complexes **2** may be formed by addition of CO to the d^9–d^9 dimers $[M_2X_2(\mu\text{-dppm})_2]$, X = Cl (**6**), and this approach is summarized in Figure 3. Approach of the carbonyl ligand at the center of the M–M bond of **6** (with X groups bent back but maintaining the M–M distance as expected for a single bond)[12] leads to a strong interaction between the filled σ-donor orbital of CO and M–M σ-bonding orbital of **6** to give a strongly bonding and strongly antibonding combination as described previously.[12] In addition the M–M antibonding orbital interacts with π^*(CO) and is sufficiently stabilized that it becomes the HOMO, shown as b_2 in column B of Figure 3.[12] There are eight roughly nonbonding 5d-orbitals in a block below b_2 and a series of vacant $2p_\pi^*$(CO) orbitals above, of which the lowest is a_1 in Figure 3. The HOMO is at high energy and the HOMO–LUMO gap b_2–a_1 is low so the molecule is not expected to be stable in this geometry. The obvious stabilizing distortion of B (Figure 3) is to move the metal atoms apart to give A (Figure 3); the antibonding interaction between the metal atoms in b_2 is then minimized as mutual overlap of the metal orbitals decreases. Of course, A is the observed structure for the complexes when M, M′ = Pt or Pd and the HOMO really is greatly stabilized by the B to A distortion as shown in Figure 3. The distortion of B to give the observed structure **1** (M, M′ = Ni) is less obvious. The carbonyl carbon slips toward M′ to give the semibridging CO, and the halide ligand X moves below M′, as shown in C (Figure 3). The HOMO is stabilized, partly because the M–M′ interaction is less antibonding, as the lower symmetry at M′ allows more mixing of d-orbitals. Bending the ligands L back from the *y*-axis to change the stereochemistry of M′ from pseudo-square pyramidal to pseudo-trigonal bipyramidal as shown in D (Figure 3) causes further stabilization of the orbital derived from b_2, while the d_{xy} orbital on M′ is destablized and becomes the HOMO. The HOMO energy and HOMO–LUMO gap are now similar for D and A. Of course, D approximates the observed structure **1a** (M = Ni).

The above calculations indicate that A = **2** and D = **1** are both viable structures, but can they explain why A is preferred for Pt and Pd but D is better for Ni? The calculations were carried out for both Pt and Ni complexes, and some results are shown in Table II. In both cases, A is calculated to be slightly more stable than D. The only indication that D might be preferable for M = Ni is that the HOMO is at marginally lower energy and the HOMO–LUMO gap is slightly higher for D when M = Ni but for A when M = Pt (Table II). Given that the LUMO is π^*(L), where L is a CO substituting for a dppm phosphorus donor, it is clear that this is of limited significance and no further speculation is warranted. In both forms, A and D, the HOMO–LUMO gap (Table II) is sufficient that the compounds are expected to be diamagnetic for both Pt and Ni, in agreement with our experimental data.[5]

Table II. Selected Parameters (*E*, Energy, eV; *Q*, Charge, e) from the EHMO Calculations

complex (M, M′)	*E*(tot.)	*E*(H)[a]	*E*(H–L)[b]	M–M′ overlap	*Q*(M)	*Q*(M′)
6 (Pt)	−1309.8	−11.85	1.82	0.28	0.24	0.24
B (Pt)	−1510.2	−10.56	0.31	0.00	0.52	0.52
A (Pt)	−1511.6	−11.62	1.67	−0.05	0.42	0.42
C (Pt)	−1510.4	−11.22	0.80	0.04	0.33	0.29
D (Pt)	−1510.6	−11.59	1.56	0.12	0.44	0.70
F (Pt)	−1509.2	−11.10	1.23	0.27	0.10	0.75
6 (Ni)	−1326.4	−12.09	2.04	0.10	0.10	0.10
B (Ni)	−1525.4	−10.63	0.44	−0.14	0.43	0.43
A (Ni)	−1526.8	−11.49	1.54	−0.11	0.37	0.37
C (Ni)	−1526.0	−11.29	1.35	−0.11	0.45	0.35
D (Ni)	−1526.4	−11.75	1.94	−0.05	0.46	0.38
F (Ni)	−1525.0	−11.26	1.59	0.09	0.04	0.55

[a] *E*(H) = energy of the HOMO. [b] *E*(H–L) = HOMO–LUMO gap.

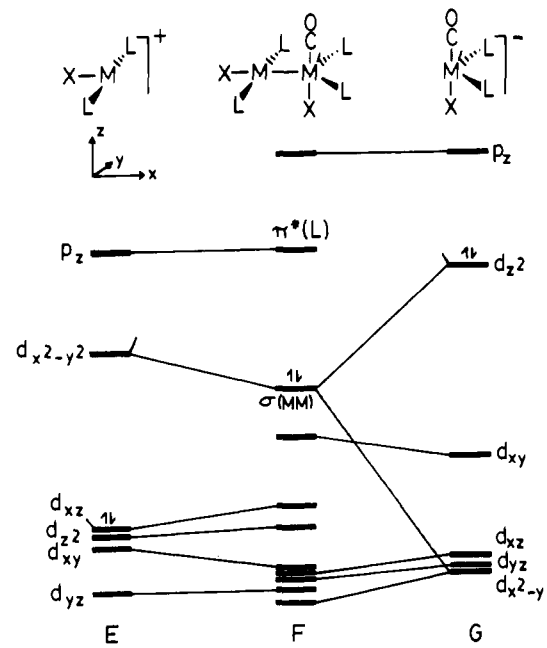

Figure 4. Molecular orbital correlation diagram for formation of the idealized square planar–trigonal bipyramidal complex F, from the fragments $[MXL_2]^+$ (14-electron) and $[MX(CO)L_2]^-$ (18-electron), with formation of a σ(M–M′)-bonding MO. The values given are for M, M′ = Pt, X = Cl, L = CO; the pattern for M, M′ = Ni is very similar.

Formation of **1** = D (Figure 3) can also be considered to occur by addition of CO to only one metal center of $[M_2X_2(\mu\text{-dppm})_2]$, whereupon that center would attain an 18-electron configuration and its stereochemistry would change from square planar (dsp^2) to trigonal bipyramidal (dsp^3), as shown in structure F of Figure 4. Complex F could also be formed by donation of electron density from an 18-electron M(0) fragment $[M'(CO)XL_2]^-$ (with geometry distorted from tetrahedral as in G (Figure 4) so as to give a filled metal-based orbital directed along the *x*-axis) to a T-shaped 14-electron fragment $[M(CO)L_2]^+$, E (Figure 4), which has a vacant acceptor orbital directed along the *x*-axis. It will be instructive to carry out calculations using the latter model, since this may give insight into the proposed donor–acceptor metal–metal bonding in **1** and related compounds.[2] A correlation diagram is shown in Figure 4. It can be seen that a strong interaction is predicted between the HOMO of G, having mostly M′ d_{z^2}, p_z character, and the LUMO of E, having mostly M $d_{x^2-y^2}$ character,

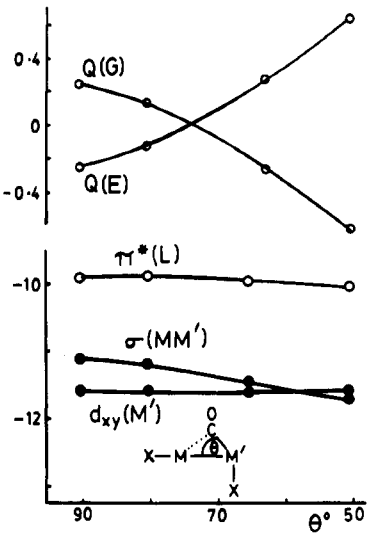

Figure 5. Bottom: Changes in the energies of three frontier orbitals {π^*(L), σ(M–M′), and d_{xy}(M′) in Figure 4}. Top: Changes in the charges on the fragments E and G, as the angle θ is reduced from the value of 90° in structure F. Values are given for M, M′ = Pt, X = Cl; very similar trends are observed for M, M′ = Ni.

Table III. Crystallographic Data for $[Ni_2Cl_2(\mu\text{-CO})(\mu\text{-dppm})_2]\cdot CH_2Cl_2$

chem formula	$C_{52}H_{46}Cl_4Ni_2OP_4$	Z	4
fw	1070.07	T	22 °C
space group	$P2_1/n$	λ(Mo Kα)	0.71069 Å
a	13.890 (1) Å	ρ(calc)	1.470 g cm^{-3}
b	18.011 (1) Å	μ(Mo Kα)	11.73 cm^{-1}
c	19.614 (1) Å	$R(F_o)$	0.038
β	99.809 (4)°	$R_w(F_o^2)$	0.051
V	4835.2 Å^3		

to give a σ(M–M′)-bonding orbital. In the process, $d_{x^2-y^2}$ character of M′ is mixed in as shown in Figure 4. This donation of charge from G to E is calculated to be sufficiently great that, when charge in F is apportioned to each fragment from which it was derived, fragment E is negatively (−0.25 e when M, M′ = Pt) and G positively (+0.25 e when M, M′ = Pt) charged. This is a classic situation for formation of a semibridging carbonyl, since sliding the carbonyl ligand of F toward M would allow it to remove charge from M by back-bonding.[14] This then leads naturally to structure **D** = **1**. A series of calculations were made as the angle θ (angle M–M′–CO, Figure 5) decreased from 90 to 50°, and some results are shown in Figure 5. As θ decreases, the orbital σ(M–M′) is stabilized while other orbitals are not much changed, and hence this distortion leads to net stabilization. The orbital character becomes complex, and includes much mixing with π^*(CO), such that in D (θ ca. 50°) it is best considered as a 3-center 2-electron bond with little computed metal–metal bonding character.[15] In addition, the computed charges on the two fragments E and G (Figure 5) decrease and then reverse as θ decreases (Figure 5). This is consistent with the expected effect of the semibridging carbonyl in removing electron density from fragment E. However, there is an equally valid way of rationalizing this effect. As θ is reduced from 90°, the fragment G moves toward its more stable tetrahedral geometry (sp^3 for a 4-coordinate d^{10} complex) and the HOMO is stabilized (moving the CO ligand away from the z-axis reduces the σ-antibonding character of d_{z^2} and allows d_{z^2} to CO π^* back-bonding, both of which effects stabilize the HOMO of fragment G). The result is that the distorted fragment G is a poorer donor and donates less charge to fragment E. The donor orbital of the distorted fragment G back-bonds strongly to CO and so becomes a mixed M′C donor rather than a more pure metal-centered donor. Whichever way one looks at this, the result is that in the case with θ ca. 50° the computed charge on fragment E is +0.63 e (M, M′ = Pt) and +0.44 e (M, M′ = Ni).[16] Thus, the original charge of −1 e on the distorted (θ = 50°) fragment

(14) Cotton, F. A.; Wilkinson, G. *Advanced Inorganic Chemistry*, 5th ed.; Wiley: New York, 1988; pp 1030–1031.

(15) Metal–metal bonding character in carbonyl-bridged complexes is debatable and has been much debated. For a recent discussion, see: Low, A. A.; Kunze, K. L.; MacDougall, P. J; Hall, M. B. *Inorg. Chem.* **1991**, *30*, 1079.

Table IV. Atomic Fractional Coordinates and Displacement Parameters for $[Ni_2Cl_2(\mu\text{-CO})(\mu\text{-dppm})_2]\cdot CH_2Cl_2$

atom[a]	x	y	z	U, Å^{2}[b]
Ni(1)	0.01585 (3)	0.17169 (2)	0.18973 (2)	0.031
Ni(2)	−0.11411 (3)	0.26069 (2)	0.22786 (2)	0.029
Cl(1)	0.13968 (8)	0.09266 (6)	0.19299 (7)	0.062
Cl(2)	−0.09758 (8)	0.24195 (6)	0.34329 (5)	0.047
Cl(3)	0.2941 (2)	0.0462 (2)	0.3580 (1)	0.143
Cl(4)	0.4254 (2)	0.1059 (2)	0.4709 (1)	0.187
P(1)	0.11320 (6)	0.26984 (5)	0.18731 (5)	0.031
P(2)	−0.04925 (6)	0.37170 (5)	0.21625 (5)	0.030
P(3)	−0.08543 (6)	0.07932 (5)	0.20719 (5)	0.030
P(4)	−0.25114 (6)	0.19555 (5)	0.20684 (4)	0.027
O(1)	−0.1098 (2)	0.2379 (2)	0.0842 (1)	0.046
C(1)	0.0500 (3)	0.3592 (2)	0.1657 (2)	0.034
C(2)	−0.2062 (2)	0.1013 (2)	0.2313 (2)	0.031
C(3)	−0.0901 (2)	0.2327 (2)	0.1448 (2)	0.033
C(4)	0.3395 (9)	0.0309 (9)	0.4377 (5)	0.238
C(A1)	0.1945 (3)	0.2903 (2)	0.2685 (2)	0.037
C(A2)	0.2588 (3)	0.3502 (2)	0.2731 (2)	0.049
C(A3)	0.3142 (3)	0.3700 (3)	0.3359 (3)	0.060
C(A4)	0.3077 (3)	0.3272 (3)	0.3935 (3)	0.074
C(A5)	0.2475 (4)	0.2676 (3)	0.3900 (2)	0.069
C(A6)	0.1889 (3)	0.2484 (3)	0.3267 (2)	0.053
C(B1)	0.1930 (2)	0.2630 (2)	0.1227 (2)	0.033
C(B2)	0.2885 (3)	0.2369 (2)	0.1418 (2)	0.041
C(B3)	0.3478 (3)	0.2284 (2)	0.0922 (2)	0.049
C(B4)	0.3136 (3)	0.2468 (2)	0.0236 (2)	0.051
C(B5)	0.2192 (4)	0.2709 (3)	0.0047 (2)	0.056
C(B6)	0.1587 (3)	0.2792 (2)	0.0537 (2)	0.048
C(C1)	−0.0009 (3)	0.4302 (2)	0.2899 (2)	0.033
C(C2)	0.0833 (3)	0.4735 (2)	0.2961 (2)	0.041
C(C3)	0.1089 (3)	0.5216 (2)	0.3516 (2)	0.047
C(C4)	0.0508 (3)	0.5278 (2)	0.4006 (2)	0.049
C(C5)	−0.0323 (3)	0.4845 (2)	0.3966 (2)	0.050
C(C6)	−0.0578 (3)	0.4355 (2)	0.3415 (2)	0.043
C(D1)	−0.1292 (3)	0.4372 (2)	0.1629 (2)	0.037
C(D2)	−0.0987 (3)	0.5066 (3)	0.1469 (3)	0.059
C(D3)	−0.1643 (4)	0.5565 (3)	0.1079 (3)	0.075
C(D4)	−0.2579 (4)	0.5362 (3)	0.0855 (2)	0.064
C(D5)	−0.2888 (3)	0.4683 (3)	0.1014 (3)	0.086
C(D6)	−0.2249 (3)	0.4185 (3)	0.1402 (3)	0.071
C(E1)	−0.0296 (3)	0.0197 (2)	0.2789 (2)	0.038
C(E2)	−0.0017 (3)	0.0525 (2)	0.3431 (2)	0.051
C(E3)	0.0440 (4)	0.0099 (3)	0.3992 (3)	0.069
C(E4)	0.0642 (3)	−0.0642 (3)	0.3887 (3)	0.072
C(E5)	0.0382 (4)	−0.0962 (3)	0.3258 (3)	0.065
C(E6)	−0.0080 (3)	−0.0541 (2)	0.2700 (2)	0.051
C(F1)	−0.1186 (3)	0.0186 (2)	0.1323 (2)	0.036
C(F2)	−0.1826 (3)	−0.0410 (2)	0.1341 (2)	0.042
C(F3)	−0.2150 (3)	−0.0820 (2)	0.0755 (2)	0.049
C(F4)	−0.1841 (3)	−0.0643 (3)	0.0139 (2)	0.054
C(F5)	−0.1208 (3)	−0.0055 (3)	0.0114 (2)	0.055
C(F6)	−0.0881 (3)	0.0364 (2)	0.0707 (2)	0.046
C(G1)	−0.3529 (2)	0.2058 (2)	0.2541 (2)	0.031
C(G2)	−0.3540 (3)	0.2624 (2)	0.3022 (2)	0.042
C(G3)	−0.4345 (3)	0.2715 (2)	0.3348 (2)	0.052
C(G4)	−0.5127 (3)	0.2230 (2)	0.3207 (2)	0.049
C(G5)	−0.5123 (3)	0.1669 (2)	0.2729 (2)	0.047
C(G6)	−0.4328 (3)	0.1583 (2)	0.2394 (2)	0.041
C(H1)	−0.3186 (2)	0.1918 (2)	0.1189 (2)	0.032
C(H2)	−0.3759 (3)	0.2533 (2)	0.0954 (2)	0.044
C(H3)	−0.4266 (3)	0.2554 (3)	0.0275 (2)	0.053
C(H4)	−0.4218 (3)	0.1967 (3)	−0.0158 (2)	0.055
C(H5)	−0.3661 (3)	0.1356 (3)	0.0072 (2)	0.055
C(H6)	−0.3148 (3)	0.1333 (2)	0.0742 (2)	0.042

[a] The atoms Cl(3), Cl(4), and C(4) belong to the solvent molecule. [b] U is the equivalent isotropic displacement parameter defined as $U = {}^1/_3\sum_{i=1}^3\sum_{j=1}^3(U_{ij}b_ib_j(\mathbf{a}_i\cdot\mathbf{a}_j))$, where U_{ij} values are the refined anisotropic displacement parameters, b_i is the ith reciprocal cell edge, and $\mathbf{a}_i$ is the ith direct cell vector.

(16) Metal–metal bonding character in carbonyl-bridged complexes is debatable and has been much debated. For a recent discussion, see: Low, A. A.; Kunze, K. L.; MacDougall, P. J; Hall, M. B. *Inorg. Chem.* **1991**, *30*, 1079.

G is only partly donated to fragment E, and so, given the reservations outlined above,[15,16] it is reasonable, although oversimplified, to regard the complex **1** as containing a donor–acceptor metal–metal bond with some residual polarity $[MXL_2]^{\delta+}[M'(CO)XL_2]^{\delta-}$.

Conclusions

The calculations show that the observed structures **1** or **2** are more stable than other possible structures such as B (Figure 3) or F (Figure 4) and that the metal–metal bonding in **2** can be considered to be of the donor–acceptor type. However, the calculations gave very similar results for the Pt and Ni derivatives and so do not explain why the different structures **2** and **1**, respectively, are adopted. For both metals, the energies of **1** and **2** are calculated to be very similar and so easy interconversion between these structures might be predicted. Since the Pt or Pd complexes **2** have high symmetry, it is not easy to determine if conversion to **1** is facile. However, the NMR data discussed above show clearly that the less symmetrical nickel complex **1a** is fluxional and, on the NMR time scale, has the symmetry characteristic of **2**. The fluxionality is still rapid at −90 °C as evidenced by the observation of a sharp singlet in the ^{31}P NMR spectrum at this temperature. The fluxionality requires an intermediate or transition state with a symmetrical bridging CO ligand, and since B (Figure 3) is expected to be significantly higher in energy, the A-frame A or **2** is the most likely candiate, as suggested in eq 2. Thus, there is experimental as well as theoretical evidence that structures **1** and **2** may readily interconvert.

Experimental Section

Nickel complexes were handled under an atmosphere of dry nitrogen by using standard Schlenk tube and drybox techniques.

$[Ni_2Cl_2(\mu\text{-CO})(\mu\text{-dppm})_2]$ (1a). A solution of $[NiCl_2(dppm)_2]$ (0.037 g) in CH_2Cl_2 (5 mL) was added to a solution of $[Ni_2(CO)_2(\mu\text{-CO})(\mu\text{-dppm})_2]$ (0.039 g) in CH_2Cl_2 (10 mL) at room temperature. Over a period of 4 h, the color of the solution changed from red-brown to green. The solution was layered with EtOH and left for 2 days, whereupon deep green-black crystals of the product precipitated. This was separated by filtration, washed with EtOH (10 mL) and then pentane (10 mL), and dried under vacuum. Yield: 89%.

The same product was obtained by reaction of $NiCl_2 \cdot 6H_2O$ (0.55 g) in EtOH (10 mL) with $[Ni(CO)_2(dppm\text{-}P)_2]$ (2.0 g) in CH_2Cl_2 (25 mL) at −78 °C. The mixture was stirred at −78 °C for 0.5 h and then at 20 °C for 0.5 h. The product was obtained by precipitation with *n*-pentane (30 mL), and a further crop was obtained by reducing the volume of the filtrate and adding more pentane (20 mL). Yield: 91%.

EHMO Calculations. Molecular orbital calculations of the extended Huckel type[17] were carried out using ICONS, with fragment MO analysis (Program ICONS. *QCPE No. 517* **1986**, *6*, 100). Weighted H_{ij} values were used throughout. Distances (Å) used were as follows: Ni–Ni, 2,62; Pt–Pt, 2.64; Ni–C, 1.79; Pt–C, 1.90; Ni–Cl, 2.24; Pt–Cl, 2.40; C–O, 1.10. These were averaged values from the X-ray structures of molecules **1** and **2**.[2,3]

X-ray Crystal Structure Analysis of $[Ni_2Cl_2(\mu\text{-CO})(\mu\text{-dppm})_2]\cdot CH_2Cl_2$ ($1a\cdot CH_2Cl_2$). Green-black crystals of this compound were obtained from CH_2Cl_2 solution. All diffraction measurements were made with graphite-monochromated molybdenum radiation and an Enraf-Nonius CAD4 diffractometer.

The unit cell constants (Table III) were determined by a least-squares treatment of the setting angles for 23 reflections with $12 < \theta < 16°$. Preliminary investigation of the diffraction pattern revealed a primitive crystal lattice and the $2/m$ Laue symmetry. Systematic absences of reflections established the $P2_1/n$ (No. 14) space group symmetry.

Intensities of reflections were measured by continuous $\theta/2\theta$ scans with the width of 0.70° in θ. The scan speeds were adjusted to give $\sigma(I)/I \leq 0.03$, subject to the time limit of 80 s. Two strong reflections were remeasured every 2 h, but their intensities showed only random fluctuations not exceeding 4% of the mean values. The integrated intensities were derived in the usual manner ($q = 0.03$)[18] and corrected for Lorentz, polarization, and absorption effects. The absorption correction was made by the empirical method of Walker and Stuart.[19] Of 15 355 reflections measured, 9403 were symmetry related and they were averaged to give 4566 independent ones and R(int) of 0.031. Only 6722 unique reflections, for which $I \geq 3\sigma(I)$, were used in the structure analysis.

The crystal structure was solved by the heavy-atom method. The positions of the nickel atoms were obtained from a Patterson function, and those of the remaining ones, including all the hydrogen atoms of **1**, from the appropriate difference electron density maps. The hydrogen atoms were included in the structural model in calculated positions (C–H = 1.08 Å) and allowed to ride on the carbon atoms to which they are bonded; only their individual isotropic displacement parameters were refined. The non-hydrogen atoms were assigned anisotropic displacement parameters. The structure was refined by block-diagonal least-squares, minimizing the function $w(|F_o| - |F_c|)^2$, where $w = \sigma^{-2}(|F_o|)$. The refinement converged at $R = 0.038$ and $R_w = 0.051$. In the final difference electron density map the function values ranged from −0.97 to +0.94 e Å^{-3}, the extreme ones being associated with solvent molecules. The final atomic coordinates are shown in Table IV.

All calculations were carried out using the GX program package.[20] Neutral-atom scattering functions were taken from ref 21.

Acknowledgment. We thank NATO for a travel grant, and R.J.P. thanks the NSERC (Canada) for financial support and Dr. N. C. Baird for helpful advice.

Supplementary Material Available: Tables SI and SII, listing anisotropic displacement parameters and bond lengths and angles (7 pages); Table SIII, listing observed and calculated structure amplitudes (22 pages). Ordering information is given on any current masthead page.

(16) Figure 5 overemphasizes the true polarity in the bridged forms ($\theta < 90°$), since the charge on the μ-CO group is attributed to fragment G only. The two metal atoms are predicted to be equally charged at θ ca. 63°, M, M′ = Pt (charge ca. +0.5 e) and at θ ca. 52° M, M′ = Ni (charge ca. +0.4 e).

(17) (a) Hoffmann, R. *J. Chem. Phys.* **1963**, *39*, 1397. (b) Rossi, A.; Howell, J.; Wallace, D.; Haraki, K.; Hoffmann, R. *J. Am. Chem. Soc.* **1978**, *100*, 3686. (c) Ammeter, J. H.; Burgi, H.-B.; Thibault, J. C.; Hoffmann, R. *J. Am. Chem. Soc.* **1976**, *98*, 3686. (d) Summerville, R. H.; Hoffmann, R. *J. Am. Chem. Soc.* **1976**, *98*, 7240.

(18) Manojlovic-Muir, Lj.; Muir, K. W. *J. Chem. Soc., Dalton Trans.* **1974**, 2427.

(19) Walker, N.; Stuart, D. *Acta Crystallogr., Sect. A: Found. Crystallogr.* **1983**, *A39*, 158.

(20) Mallinson, P. R.; Muir, K. W. *J. Appl. Crystallogr.* **1985**, *18*, 51.

(21) *International Tables for X-Ray Crystallography*; Kynoch: Birmingham, England, 1974; Vol. 4, pp 99, 149.